Turkish J. Eng. Env. Sci.
31 (2007) , 403 – 413.

A Simple Methodology for Sensor Driven Prediction of Upward Flame Spread

Adam COWLARD, Lukas AUERSPERG
BRE Centre for Fire Engineering, School of Engineering and Electronics, University of Edinburgh, EH9 3JL, Scotland, U.K.
e-mail: Adam.Cowlard@ed.ac.uk
Jean-Baptiste RICHON
Laser and Imaging Sciences Ltd, Edinburgh, Scotland, U.K.
Guillermo REIN, Stephen WELCH, Asif USMANI, Jose L. TORERO
BRE Centre for Fire Engineering, School of Engineering and Electronics, University of Edinburgh, EH9 3JL, Scotland, U.K.

Received 03.12.2006

Abstract

Mathematical models of flame dynamics in natural fires require solving complex mechanisms and involve large and small, length and time scales. These models demand heavy resources and computational time periods that are far greater than the time associated with the processes being simulated (hours to model seconds). If comprehensive computational models are ever to be used to estimate, forecast and understand fire growth in support of emergency response, the computational time has to be shorter than the event itself: super-real time. A mechanism to achieve these computational speeds is by means of theoretical models steered by continuous calibration against sensor measurements. In this paper, the concept of super-real time predictions steered by measurements is studied in the simple yet meaningful scenario of upward flame spread. Experiments have been conducted with PMMA slabs to feed sensor data into a simple analytical model. The sample is 150 mm wide, 40 mm thick and 200 mm tall. CCD cameras and thermocouples embedded into the solid provide estimates of the evolution of the pyrolysis front. Heat flux gauges estimate the radiative heat flux from the flame to the solid. Flame height is measured with CCD cameras, and a PIV system is used to characterize the flow field. A simple algebraic expression from the literature linking flame spread, flame characteristics and pyrolysis evolution has been used to model upward flame spread. The measurements are continuously fed to the computations so that projections of the flame spread velocity can be established at each instant in time, ahead of the real flame. It was observed that as the input parameters in the analytical models were optimised to the scenario, rapid convergence between the evolving experiment and the predictions was attained.

Key words: Flame Spread, Sensor Driven Prediction, PMMA.

Introduction

This research is approached in the context of studies of fire dynamics in enclosures and how to provide predictions to aid emergency response. FireGrid (FireGrid, (web)), is a large-scale research project that aims to provide a tool to aid in real-time emergency response. One main focus of the project is structures in fire.

Current computational models of flame dynamics in natural fires involve solving coupled flow, thermal and chemical mechanisms involving length-scales ranging from metres to millimetres, and time-scales from minutes to milliseconds. These models demand extensive computational times that are far greater than the time associated with the phenomena themselves (hours to model seconds). Simulation times can only be significantly reduced by the

use of immense, and rarely available, computer resources, thus, it is virtually impossible to provide real-time predictions for emergency response situations. If comprehensive computational models are ever to be used to estimate, forecast or understand fire growth in support of emergency response, a simple, robust, effective approach is required to vastly reduce the computational time and accelerate predictive simulations to speeds beyond what computers will be expected to attain in the near future. The proposed mechanism to achieve these elusive computational speeds is by means of theoretical models by continuous sensor measurements.

FireGrid aims to develop a methodology to enable the provision of super-real time predictions governed by live sensor information from the evolving hazard to the emergency responders. Emphasis is given to the impact from the fire environment on the structures (*i.e.* heat fluxes) and evacuation (*i.e.* tenability conditions and toxicity) and the coupling of predictive tools associated with these features.

A major challenge to the FireGrid methodology is the real-time integration of sensor data into the fire modeling process. This idea is similar to the process of Data Assimilation (Nichols, 2003) (Schlatter, 2000) in the field of meteorology, but the characteristic time scale in fire applications is in the order of minutes and not days. FireGrid aims to provide predictions even when fundamental changes take place in an evolving emergency scenario. For example, if a window breaks or a sprinkler is activated during a fire in a building, the flame dynamics are significantly modified therefore the system should respond to this change by readjusting its predictions to the new conditions. This concept is illustrated in Figure 1, where sensor data is assessed and then continually reassessed to recreate the fire environment and steer the computations.

This paper uses a flame propagating upwards over a vertical slab of PMMA to test the potential of using a combination of sensors and simple analytical models to achieve adequate super-real time predictions of the rate at which a flame spreads. This particular configuration has been chosen because it represents a realistic fire problem and has been well studied in the past (Fernandez-Pello, 1977), thus reference data exists to benchmark the present measurements.

For the present experiments, sensor information is converted into measurements of the different physical processes, including the flame height evolution in time. Based on these measurements, a model provides a prediction of the time evolution of the flame height. Subsequent incoming sensor data is compared to the prediction at different analysis times and corrections / recalibrations are applied when divergence is larger than the expected experimental error. The continuous use of sensor data to check the modeling accuracy allows for improved model predictions as more experimental information becomes available. Moreover, it is required that the methodology be robust enough to capture significant changes in the environment (Figure 1).

Analytical Model

A simple case of vertical upward flame spread is chosen as the initial step to validate the concept of super-real time predictions. Upward flame spread is chosen because it is simple enough to be plausible as a proof-of-concept and yet still a meaningful fire scenario. Experiments are conducted with PMMA slabs to feed measurements into a simple analytical model.

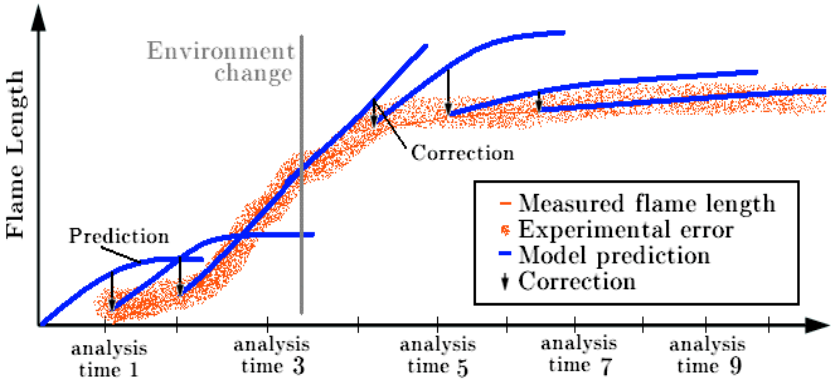

Figure 1. Conceptual representation of the data assimilation process and the sensor steering of model predictions.

PMMA is one of the best characterized materials for flame spread. Although downward spread may be easier to model, upward spread includes a proper definition of the pyrolysis length, thus adds a measurable variable to the analysis. A simple algebraic expression from the literature (Fernandez-Pello, 1995) linking flame spread, flame characteristics and pyrolysis is used to model the process. The following expression is derived for thermally-thick materials:

$$V_f = \frac{4c\left[(c_1 k_g \rho_g c_p u_\infty / l_p)^{1/2}(T_f - T_p) + \dot{q}''_{fr} + \dot{q}''_e - \dot{q}''_{rs}\right]^2 l_p}{\pi k_s \rho_s c_s (T_p - T_0)^2} \quad (1)$$

All variables are defined in the nomenclature. The constants and variables within the model can be classified into four categories: material properties, scenario-specific dimensional constants, scenario specific non-dimensional parameters and sensor measured quantities that vary with time.

The thermal properties present in Equation (1) are assumed to be constant. These vary with temperature but it is assumed that this variation is spatial and that the distribution does not significantly change in time. Equation (1) was developed for forced flow concurrent flame spread thus cannot be applied directly to upward flame spread. The differences are all concentrated in the definition of u_∞. Here u_∞ will be derived from measurements, thus there is no need to include an expression that accounts for buoyancy. Temperatures and heat fluxes will be measured directly.

The flame height is generally assumed to be directly proportional to the pyrolysis length (Equation (2)), therefore, given the knowledge of the evolution of the pyrolysis and flame lengths, the non-dimensional parameter c can be directly obtained from Equation (2).

$$\frac{l_f}{l_p} = c \quad (2)$$

The final unknown in the Fernandez-Pello model (Equation (1)) is the non-dimensional parameter c_1. This parameter can be obtained directly using Equation (1), being the only unknown at any instant in time over the data collection period. Experiments show that c_1 varies in time so a fit should be applied to this parameter in order to predict its future value.

Once values and trends for all constants and time variant parameters have been established, Equation (1) can then be used to predict the evolution of the flame spread velocity for the rest of the test. This prediction is continuously checked against incoming data and if at any stage, the prediction and reality are found to vary significantly, this process is repeated.

Most sophisticated CFD-based fire prediction tools compute gas-phase parameters (properties, velocity fields and temperatures) but still use a simple approach to flame spread that is consistent with the present analysis (N.I.S.T., (web)). Possible modifications and simplifications to current modeling tools that will allow for faster computations will most likely resort to the substitution by measurement of gas-phase parameters, via a process of data assimilation. Nevertheless, this requires the integration of pre-computed scenarios, sensor data and computations that is the subject of further effort. Here, because the model is a simple algebraic expression, the integration of pre-computed scenarios is trivial and all the information is contained within the calibration constants.

Experimental Procedure

The experimental setup, detailed below, is designed in such a way that the sensor output can provide the majority of the analytical model's inputs. This initial setup also aimed to replicate as closely as possible the conditions, and therefore the results, described by Fernandez-Pello, (1977). In this way the techniques for sensing, data processing, and data interpretation can be validated without the need to repeat experiments excessively. The flame spread process takes place on a 40 mm thick, 200 mm high, 150 mm wide, vertically inclined PMMA slab. A horizontal line of flame is initiated by means of a Nichrome wire, embedded across the bottom of the face of the slab. A current is passed through the wire causing resistive heating and pyrolysis of the PMMA. A pilot flame is used to ignite the resulting combustible mixture. The flame front propagates to the top of the slab, whereupon it is extinguished.

A line of 19 thermocouples are embedded 1 mm behind the slab's exposed surface, along its vertical centreline, at 10 mm spacing and used to track the progression of the pyrolysis front. Visual confirmation is obtained by filming the production of pyrolysis bubbles through the rear of the sample. Flame temperature is monitored by 9 thermocouples in the gas phase. Five thermocouples come through the sample from the rear, offset 50 mm from the vertical

centreline, at heights of 20, 60, 100, 140, and 180 mm above the initiation point. The final four are positioned in an evenly spaced rack extruding from the centre of the top of the sample. The flame height is post-processed from footage from two CCD cameras filming from the front of the sample, one close to the sample giving greater detail of the flame in the region of the PMMA and the other further away, showing the growth beyond the top of the slab. A good correlation is found between the two sets of data produced in the early stages of growth. A frame rate of 29 frames per second is used. Each frame is converted from colour to a $0 - 255$ scale and binarised about a threshold to eliminate background noise. A sensitivity analysis associated to the threshold choice was conducted before defining the specific value of 100 for the threshold. Five seconds worth of frames can then be averaged to produce a pixel value between 0 and 1. The image is re-binarised about a threshold of 0.5 (50% presence probability) which gives values of 1 where the flame has been present for more than 50% of the 5 second period and 0 where it has not. The height of this block of "ones" is measured in pixels, converted to millimetres and this value is then taken as the flame height.

Measurement of the flame-induced radiant heat flux to the PMMA surface is achieved through development of a type of Thin Skin Calorimeter heat flux gauge. The Thin Skin Calorimeters consists of a copper disc, 2 mm thick and 20 mm in diameter. A narrow angled hole is drilled through the thickness of the disc, into which is inserted a Type K thermocouple. The hole is then closed around the thermocouple bead. The disc is tightly fitted into a flat-bottomed hole of identical dimensions with the thermocouple wire exiting via a 3mm diameter hole to the rear face of the PMMA slab. The face of the disc is then painted black in order to provide an emissivity close to one.

Five calorimeters are placed in a vertical line 50 mm from the centre line of the PMMA slab at heights of 20, 60, 100, 140, and 180 mm above the ignition line. A one-dimensional energy balance is used to calibrate the discs and subsequently compute the incident heat flux to the discs surface as a function of the temperature measured in the disc. In order to define this relationship, the proportion of the energy stored in the disc that is subsequently lost through conduction to the PMMA surroundings can be quantified experimentally. The Thin Skin Calorimeters are calibrated using a radiant panel and with the PMMA substrate. The result is an expression of conductive losses as a percentage of the incident radiative heat flux varying with temperature. With this relationship an expression can be developed defining q_{fr} as a function of solid and flame temperatures.

A Particle Image Velocimetry (PIV) system is used to obtain the ambient velocity U_∞ from a gas-phase ambient velocity vector profile. A Neo 65-15 twin cavity Nd:YAG laser from Oxford Lasers fitted with a light sheet generation optics is used for measurement plane illumination. Image acquisition is performed by two Firewire CCD cameras with a 1392x1040 pixel^2 resolution. One advantage of a two-camera configuration when acquiring particle images in radiant flames is the ability to set very short exposure times on both images in each PIV image pair, thereby minimising flame-induced background noise during analysis. No bandpass filters have been used on the optics. The PIV system synchronisation and image recording is performed with R&D Vision HIRIS software and electronics. VidPIV software from ILA is used for image analysis, with resulting vector maps then exported to Matlab for post-processing and presentation. Titanium Dioxide particles are used for seeding the flow. The particles have a nominal diameter in the 0.5 - 1 μm range and are introduced through a purpose-designed solid particle seeder. The task of uniformly distributing seeding particles while minimising impact on the observed flow presents a particular challenge in free convection flows such as the one studied here, due to the low velocities and weak mixing. Various seeding injection schemes have been trialed in a bid to address this issue, the best-performing one being a long narrow slit covered with fine metallic mesh.

The entire system is housed in a versatile frame of aluminium extrusion. The PMMA itself is housed in a steel frame similar to that used by Fernandez-Pello, (1977) and insulated from its supports using fire board.

Results and Analysis

To define the pyrolysis front evolution, data delivered by the 19 thermocouples measuring sub-surface temperature down the centreline of the PMMA and images from the back of the PMMA from a network of cameras are used.

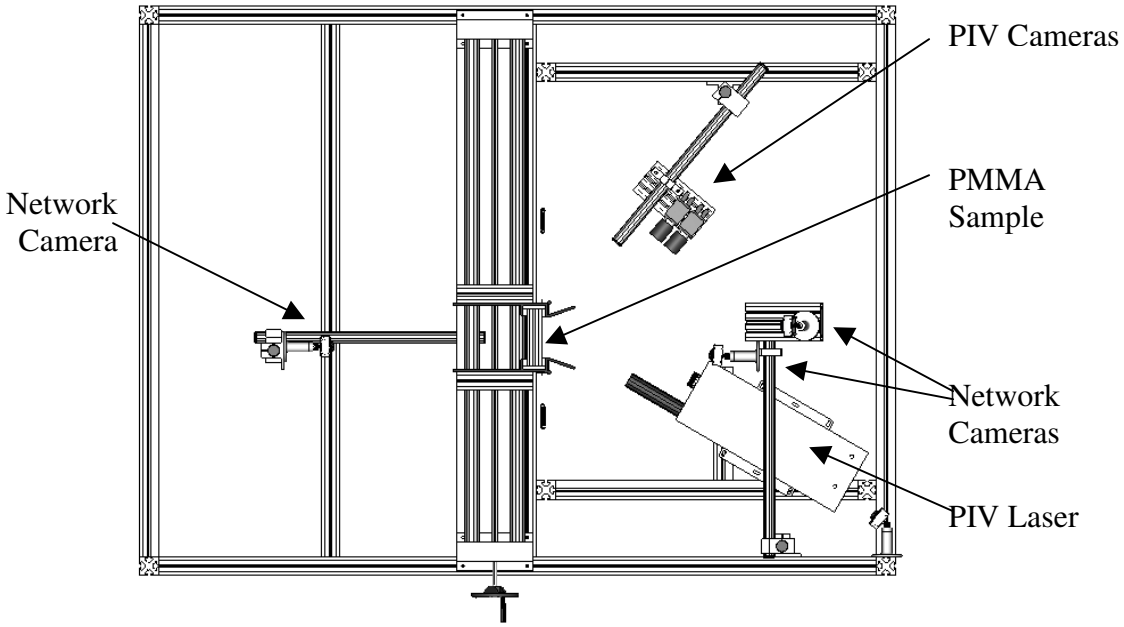

Figure 2. Plan view of experimental setup.

It has been shown that the pyrolysis temperature is not one fixed value as the reaction rate of the solid differs significantly when conditions are changed. Also it appears that the formation of pyrolysis "bubbles" occurs in a two-step reaction where oxygen availability on the surface plays an important role. All these effects mean that the pyrolysis reaction of PMMA occurs over a range of temperatures of approximately 200 to 350 °C (Dakka, et al, 2002). This temperature range is defined for the surface of the fuel whereas the sensing method employed here gives readings at a depth below the surface, thus the measurements appear lower due to thermal lag. An estimate of the variation of the sub-surface temperature with respect to the proven surface temperature range is not easy to establish and thus a simple approach is followed to determine the temperature indicated by the embedded thermocouples corresponding to the early stages of pyrolysis at the surface.

Various isotherms are plotted against the length scale and time post ignition at which they were detected in the experiment. Secondly, times and heights are recorded of the evolution of pyrolysis bubbles as observed visually from camera footage. This data is plotted alongside the isotherms in order to show which thermocouple response most closely corresponds to the visual data. Figure 3 below shows that the visually recorded data coincides strongly with the 80 °C temperature measurements. This can be seen repeatedly throughout all the experiments conducted.

The gradient of the isotherms represents the rate of evolution of temperature up the PMMA and it is noted that in the range of 60 °C to 140 °C these lines are almost parallel, with a constant spread rate in the range of 0.5 to 1.0 mm/s. This suggests that the pyrolysis evolution also has a similar rate of spread.

The readings of the thermocouples have relatively large scatter. The thermocouples are inserted from the back of the PMMA slab into holes and held in place by wire clips. It is not possible to guarantee for all thermocouples to be in exactly same position relative to the surface of the PMMA due to the accuracy of the hole depths and any PMMA residue at the ends of the holes. It is possible that some of the beaded heads of the thermocouples become bent in various directions when inserting them. Also differences in cavities of air between the ends of the holes and the thermocouples can influence the readings.

Figure 3 also shows the experimental results reported by Fernandez-Pello, (1977). Results for the evolution of the pyrolysis length obtained here show a close resemblance validating the sensing technique and the interpretation of the data.

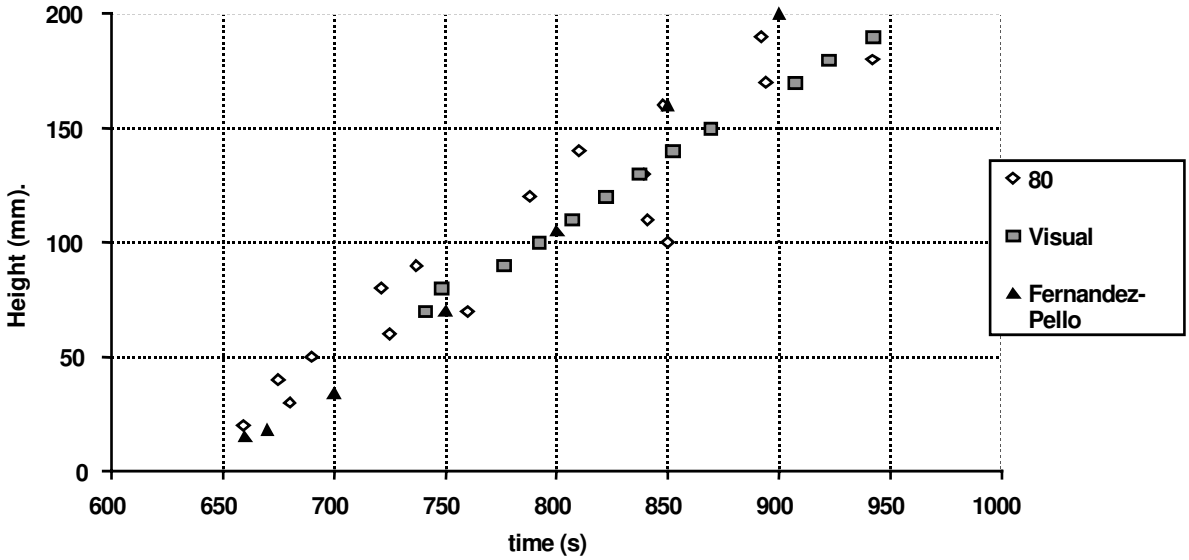

Figure 3. Visually observed arrival of pyrolysis bubbles at various heights (mm) of PMMA slab (*Visual*) in comparison with reading of 80 °C (80) and results from the literature (*Fernandez-Pello*, 1977).

The flame height indicates an almost linear growth rate until the entire face of the PMMA is ignited, slowing slightly when the flame becomes more turbulent (Figure 4). The results show a growth rate of approximately 1.1 mm/s, again comparing well with those of Fernandez-Pello, (1977). The experimental results are highly repeatable.

A characteristic flame temperature is measured by gas-phase thermocouples at various heights on the face of the PMMA, protruding 10mm from the solid surface. The flame temperature can be seen to be reasonably steady once the flame envelops the thermocouples, shown in Figure 5. The temperature decreases at the lower thermocouples as the flame grows and moves closer to the PMMA surface near its base. Once the readings reach a peak, an average temperature can be gauged. In this case the value T_f is set to 710 °C. It is important to note that this is not truly a flame temperature but a characteristic value suitable for heat transfer calculations and thus for the model presented in Equation (1).

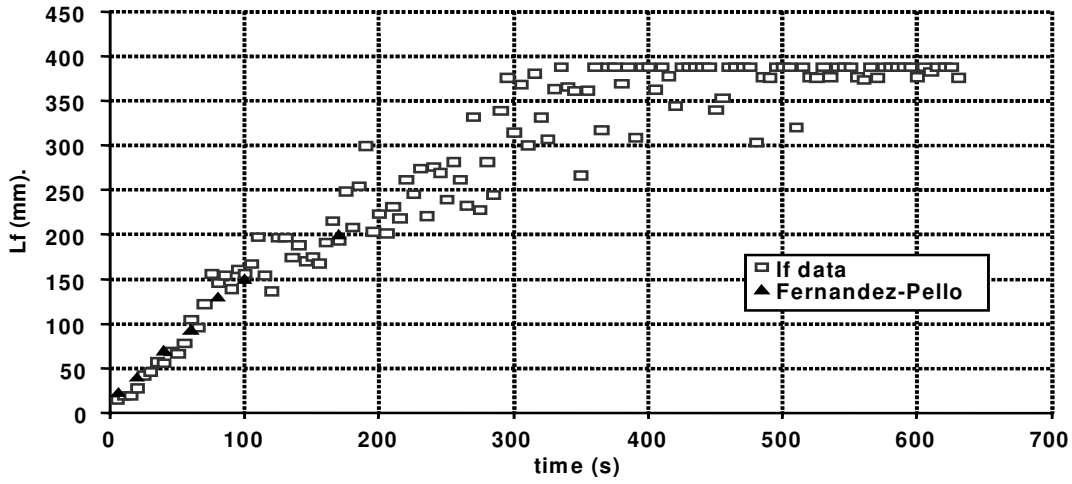

Figure 4. Flame height, l_f vs. time (*lf data*) and results from the literature (*Fernandez-Pello, 1977*).

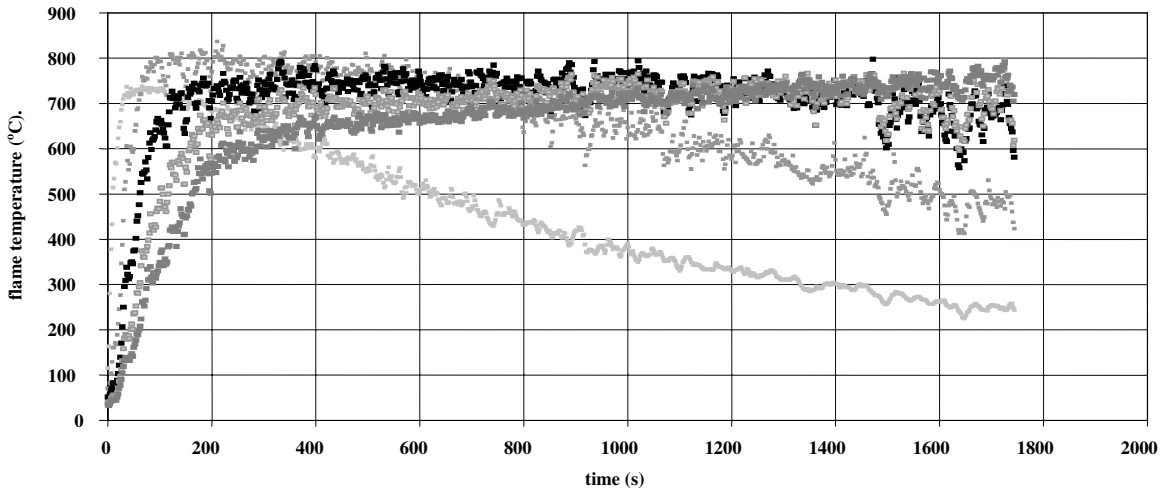

Figure 5. Evolution of the flame temperature with time.

The evolution of the ambient flow velocity is established through use of Particle Image Velocimetry (PIV). Measurements are taken during experiments at a rate of two Hertz producing velocity vector maps. The characteristic velocity was obtained within a window placed at the leading edge of the flame. This region was deemed to be consistent with the definition of u_∞ provided by Fernandez-Pello, (1995).

Figure 6 shows a typical velocity vector field obtained during the experiments. From this map a characteristic velocity, u_∞, must be obtained as this is required by Equation (1). u_∞ is taken as the maximum vertical component of the velocity vectors. The evolution of this component with time is shown in Figure 7 below. The ambient flow velocity data are noisy but the average over time is fairly constant at around 150 mm/s.

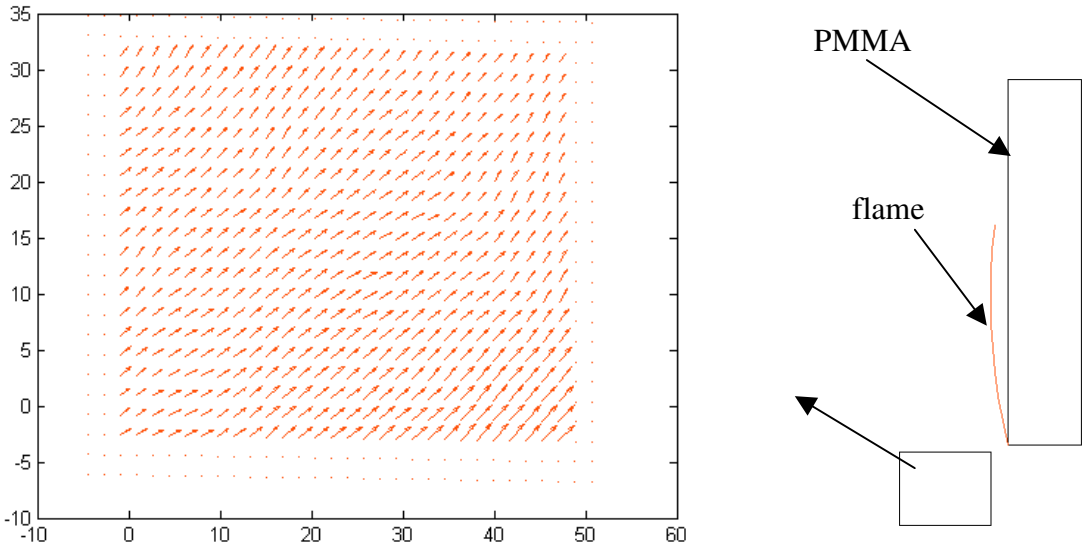

Figure 6. Typical velocity vector map, coordinates in mm.

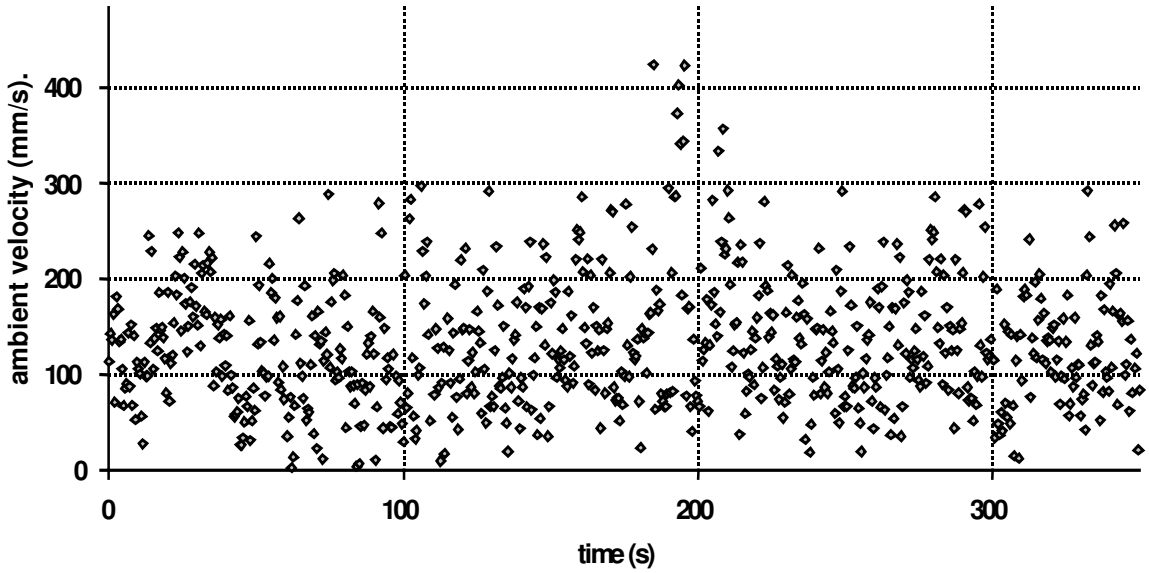

Figure 7. Evolution of the ambient flow velocity with time.

The adopted flame spread model considers conduction from the surface through the depth of the PMMA as negligible and so neglects its contribution. The results obtained in this study indicate that initially, as the flame is small and laminar and the surface ahead of the pyrolysis front is still relatively cool, the proportion of heat flux to the surface that is then conducted away through the solid is comparable with the incident radiative flux. In order to assess the evolution of q_{fr}, the values recorded by flux meters in the region between the flame tip and pyrolysis front are averaged. The characteristic value of q_{fr} for the first time period is taken as the average of those results over that time period. Initially this value is negative and so is set to zero, signifying a balance between the radiative flux to the surface and the conductive losses from it. Later on this value rises to approximately 3 kW/m^2. It is clear that the heat fluxes recorded by the calorimeter include the conductive heat transfer through the solid phase, therefore the computed values are lower than those previously reported in the literature. It is important to note that because the flame spread model neglects this term, for this study quantification of in-depth conduction has not been done.

Super-Real Time Predictions

Analysis of the ambient air velocity shows a near constant average velocity of approximately 150mm/s throughout the early stage of the spread process. This indicates a constant spread rate up to the current time so consequently a linear fit is applied to the initial pyrolysis front evolution data which gives an initial approximation of 0.61 mm/s. A linear relationship is also established for the flame height and the value of the unknown non-dimensional constant c is established as 1.6. This value subsequently falls as more data becomes available to approximately 0.95. The initial value of q_{fr} is estimated as 0 based on the data available to the model at that time which accounts for the in-depth conductive losses from the PMMA surface. Other values required for the model, supplied by sensors are T_{flame} at 710 °C and T_0 at 20 °C. This leaves the parameter c_1 which can now be resolved at each instant in time. With all of the model's criteria, both constant values and time variant established, the prediction can then be made of the future evolution of the spread rate. Once a prediction is made the subsequent incoming data points are checked against the prediction and when they appear to deviate significantly from this, the same process can be repeated to re-calculate the constants and time-dependent variables.

If the environmental conditions are shown by sensor readings not to have altered significantly from the beginning of the event until the current time, the spread velocity for the entire experiment is reassessed. Should it be deemed that environmental conditions have changed, the new evaluation would

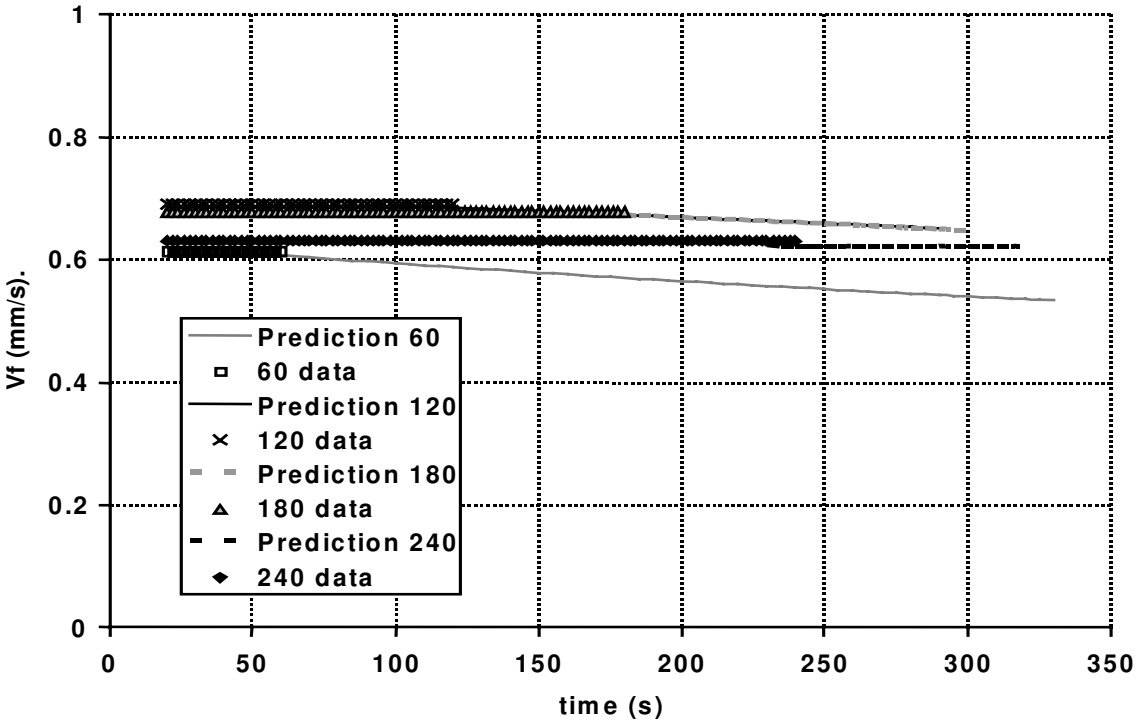

Figure 8. Evolving flame spread prediction obtained from 60 seconds of data (*60 data*), 120 seconds of data (*120 data*), 180 seconds of data (*180 data*), and 240 seconds of data (*240 data*). Predictions shown by lines labelled "Prediction XX".

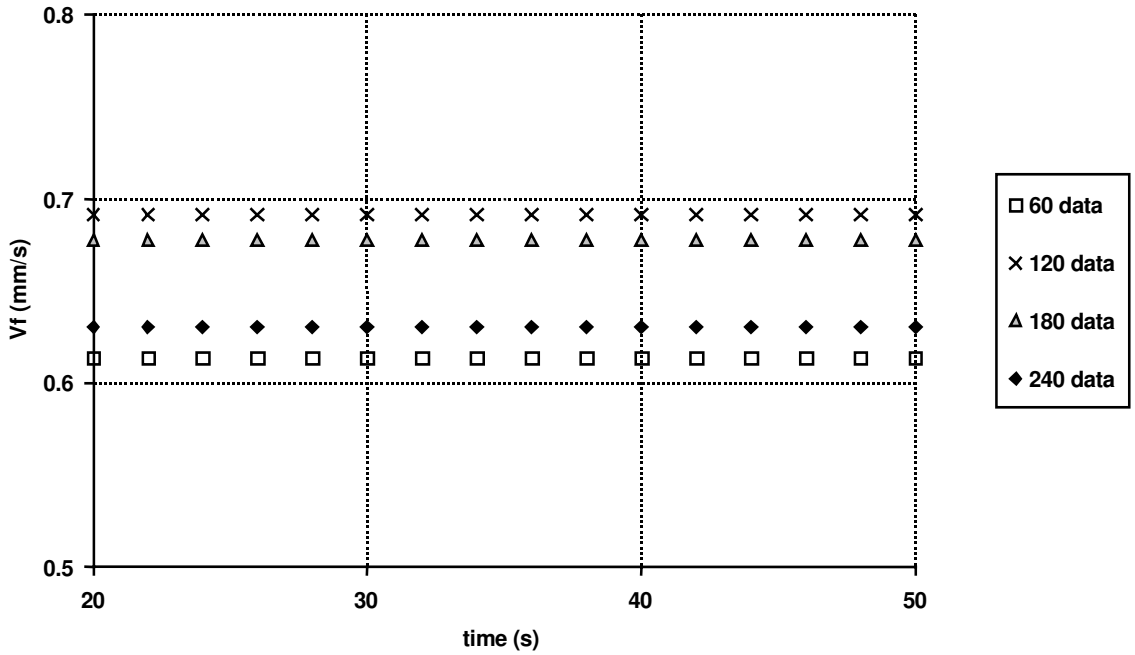

Figure 9. Close up of Figure 8 showing the change in spread rate estimation given 60 seconds (60 data), 120 seconds (120 data), 180 seconds (180 data), and 240 seconds (240 data) of data.

focus on the data collected since the time of that change. Given that the environmental conditions are deemed not to have varied, and with more isotherm data now available from which to assess the spread rate, a more accurate fit is made to the pyrolysis front evolution data. A better valuation of the spread rate from the start of the experiment to the present is made and the process repeats itself to form a more accurate prediction. As time progresses and more data is created, the predictions can be seen to converge (Figure 8). The variation in the estimation of spread rate from the pyrolysis front data as more isotherm data points are reached is shown in greater detail in Figure 9.

Conclusions

The results demonstrate the concept of super-real time predictions made from sensor data, using simple optimisation techniques and simple analytical models. As more sensor data is received, the prediction generated by the technique improves. A flexible and versatile experimental platform has been constructed with which to further develop the methodology. This experimental setup was designed in part to mimic the test results of Fernandez-Pello, (1977) thereby showing that the sensing techniques and the interpretation of the data produced to be accurate. In general the results compare favourably with those in the literature and show good repeatability.

Acknowledgments

Financial support from the BRE Trust for Adam Cowlard is gratefully acknowledged. The work reported in this paper has formed part of FireGrid, www.firegrid.org. This

research has been funded by the Technology Strategy Board along with contributions

from the other partners in FireGrid.

Nomenclature

c	Non dimensional ratio of l_f / l_p
c_1	Non-dimensional parameter
c_p	Specific heat of gas
c_s	Specific heat of solid
k	Thermal conductivity
l_f	Flame length
l_p	Pyrolysis length
q_e	External radiant flux
T_0	Initial solid temperature
T_f	Flame temperature
T_p	Pyrolysis temperature
u_∞	Ambient flow velocity
V_f	Flame spread rate
ρ	Density

Subscripts

g	gas
s	solid
q_{fr}	Radiant flux from the flame to the solid
q_{rs}	Re-radiation from the solid surface

References

Ahmad T, Faeth G.M, "Turbulent Wall Fires", 17^{th} Symposium (Int.) on Combustion, The Combustion Institute, 17, 1149-1160, 1979.

Alston J, "Room/Corner Fire Calibration Data: Marine Composite Screening Specimens", PhD Thesis, Worcester Polytechnic Institute, 2004.

Amundarain A, "Assessment of the Thermal Efficiency, Structure and Fire Resistance of Lightweight Building Systems for Optimised Design", PhD Thesis, University of Edinburgh, 2007.

Dakka S, Jackson G, Torero J, "Mechanisms controlling the Degradation of POLY(METHYLMETHACRYLATE) Prior to Piloted Ignition", Proceedings of the Combustion Institute, 29, 281-287, 2002.

Fernandez-Pello A.C, "Upward Laminar Flame Spread Under the Influence of Externally Applied Thermal Radiation", Combustion, Science and Technology, 17, 87-98, 1977.

Fernandez-Pello A.C, "The Solid Phase, Chapter 2, Combustion Fundamentals of Fire", Ed. G. Cox, Academic Press Ltd, ISBN 0-12-194230-9. 1995.

Hasemi Y, "Thermal Modelling of Upward Wall Flame Spread", Fire Safety Science, Proceedings of the First International Symposium, 1, 87-96, 1985.

Ingason H, De Ris J, "Flame Heat Transfer in Storage Geometries", Fire Safety Journal, 31, 39-60, 1998.

Nichols N.K, "Data Assimilation: Aims and Basic Concepts", Data Assimilation for the Earth System, Swinbank R, Shutyaev V, Lahoz W.A (eds), Kluwer, Dordrecht, 2003.

Quintiere J, Harkleroad M, Hasemi Y, "Wall Flames and Implications of Upward Flame Spread", Combustion, Science and Technology, 48, 191-222, 1968.

Schlatter T.W, "Variational Assimilation of Meteorological Observations in the Lower Atmosphere: a tutorial on how it works", Journal of Atmospheric and Solar-Terrestrial Physics 62, 10-57, 2000.

Firegrid http://www.firegrid.org

N.I.S.T. Fire Dynamics Simulator and Smokeview, http://www.fire.nist.gov/fds/